GEOLOŠKI ANALI BALKANSKOGA POLUOSTRVA
Volume 84 (1), July 2023, 5–16
–
https://doi.org/10.2298/GABP230301003B
Original scientific paper
Оригинални научни рад

Infrared spectra study of the Moslavačka Gora (Croatia) tourmalines O-H stretching region: inference of fluid involvement in the Late Cretaceous igneous evolution of a complex Adria – Europe convergence zone

Dražen Balen[1] & Zorica Petrinec[1]*

Abstract. Infrared spectra (IR) in the O-H stretching region were recorded for natural tourmalines from the magmatic and magmatic-hydrothermal systems of Moslavačka Gora (Croatia). Samples of disseminated tourmaline (schorl) representing magmatic products were collected from leucogranite. Nodular tourmaline (intermediate members of the schorl-dravite series) from two-mica granite represents a magmatic-hydrothermal mineral related to the final stage of granite crystallization. IR spectra of the typically disseminated tourmaline show four sharp O-H stretching bands: 3643, 3633, 3550, and 3484 cm^{-1}, while typical nodular tourmaline shows spectra with asymmetric and relatively broad O-H stretching bands on 3635 and 3554 cm^{-1} with shoulders at the higher and lower wavenumber side. The broadening in the lower wavenumber region of nodular tourmaline compared to disseminated tourmaline indicates a higher water content in the nodular type. At the same time, the observed shifts between the corresponding bands can be explained by the shortening of the O-H_1 and O-H_3 distances, which can be attributed to different genetic and/or evolutionary processes. According to the models applicable to the Moslavačka Gora, disseminated tourmaline from the leucogranite can be considered a typical magmatic (pegmatitic) product and a standard accessory phase of the leucogranite. The origin of nodular tourmaline, which was the last mineral to crystallize in the evolved Late Cretaceous granitic system of Moslavačka Gora, is attributed to the interaction of a fluid phase from the residual granitic melt with the fluid originating from the wall-rock in the low-pressure crustal setting, which was accompanied by relatively rapid cooling. This interaction resulted in an increased dravite content of the nodular tourmaline and is reflected in the observed IR spectral features.

Key-words:
IR spectra, tourmaline, schorl, dravite, Moslavačka Gora.

Апстракт. Инфрацрвени спектри (IR) турмалина из магматског и магматско-хидротермалног сустава Мославачке горе (Хрватска) снимљени су у подручју O-H растезања (stretching). Узорци дисеминираног турмалина шерла (schorl) прикупљени из леукогранита представљају магматски минерал. Турмалин из нодула (члан серије

[1] Division of Mineralogy and Petrology, Department of Geology, Faculty of Science, University of Zagreb, Horvatovac 95, HR–10000 Zagreb, Croatia
* Corresponding author: zorica.petrinec@geol.pmf.unizg.hr

schorl-dravit) у двотињчастом граниту представља минерал настао у магматско-хидротермалном циклусу унутар завршне фазе кристализације тог гранита. IR спектар типичног дисеминираног турмалина показује четири уске O-H врпце настале услијед растезања и то на 3643, 3633, 3550 и 3484 cm^{-1}, док спектар типичног турмалина из нодула показује асиметричне и релативно широке врпце O-H растезања на 3635 и 3554 cm^{-1} с проширењима на вишим и нижим валним бројевима. Проширење према нижем валном броју опажено код нодуларног турмалина указује на виши садржај воде у нодуларном типу турмалина у успоредби с дисеминираним турмалином, док се уочени релативни помаци између одговарајућих врпци могу објаснити скраћивањем O-H$_1$ и O-H$_3$ размака, што се може приписати различитим генетским и/или еволуцијским процесима. Према петрогенетским моделима који се примјењују за Мославачку гору, дисеминирани турмалин из леукогранита се може сматрати типичним магматским (пегматитским) продуктом и уобичајеном акцесорном фазом леукогранита. Поријекло нодуларног турмалина, који је кристализирао као посљедњи минерал у еволуираном каснокредном гранитном суставу Мославачке горе, приписује се међудјеловању флуидне фазе из резидуалне гранитне магме с флуидом поријеклом из околних стијена у увјетима ниског тлака у плиткој кори, што је праћено релативно брзим хлађењем. Ово међудјеловање резултирало је повећаним садржајем дравита у саставу нодуларног турмалина и одражава се у уоченим IR спектралним значајкама.

Кључне речи:
IR спектри, турмалин, шерл (schorl), дравит, Мославачка гора.

Introduction and geological setting

The Moslavačka Gora (MG) crystalline in northern Croatia, like the surrounding basement of the Pannonian Basin, consists of various igneous and metamorphic rocks. The igneous rocks are predominantly granitoids, while the surface exposures of the metamorphic rocks include medium- to high-grade metamorphic lithologies (Korolija & Crnko, 1986; Korolija et al., 1986; Crnko, 1990; Crnko & Vragović, 1990; Pamić, 1990) – Fig. 1. The present large-scale regional geological interpretation locates MG crystalline in the Sava (-Vardar) Zone (Pamić, 1993, 2002; Spahić, 2022; Spahić & Gaudenyi, 2022) or Sava Zone (Schmid et al., 2008, 2020), i.e., in the suture zone between Adria microplate and Europe, marking the southwestern margin of the Pannonian Basin towards the Dinarides (Fig. 1a).

The MG granitoid pluton comprises roughly 110 km^2 of exposed crystalline and hosts several types of granitic rocks, as indicated by field, petrographic, and geochemical studies (e.g., Pamić, 1990). Geochemistry reveals the general predominance of two major granitoid varieties: two-mica granite and leucogranites. Two-mica granite (biotite>>muscovite) is the most common type, frequently cut by the two leucogranite subtypes (coarse-grained and fine-grained, both containing muscovite). All granite types have similar mineral composition and S-type chemical signatures according to criteria of Chappell & White (1974), such as relatively low Na_2O (2.71–3.85 for two-mica granite vs. 2.58–4.67 wt. % for leucogranite) and the corresponding K_2O content (3.65–6.01 wt. % vs. 3.47–7.10 wt. %), strong peraluminosity (ASI (molar $Al_2O_3/(CaO+Na_2O+K_2O)$) =1.1–1.2 vs. 1.1–1.6) and high SiO_2 content coupled with low concentrations of FeO^{tot} and MgO (with slightly different Fe-numbers: for two-mica granite 62–63 vs. 69–89 for leucogranite). Trace elements characteristics, and exceptionally high LIL (large ion lithophile) trace element concentrations, corroborate the above conclusion. Chondrite-normalized REE patterns for two-mica granites are moderately flat and fractionated ($(La/Yb)_N$=4.33–9.67), with a slight enrichment in LREE and a strongly negative Eu anomaly (Eu/Eu^*=0.41–0.56 where $Eu/Eu^*=Eu_N/\sqrt{Sm_N*Gd_N}$), ΣREE=70.34–121.38 ppm. Similarly, chondrite-normalized REE patterns for leucogranites are characterized by the presence of two subgroups of flat patterns ($(La/Yb)_N$=1.88–2.33 and 2.10–2.67) with pro-

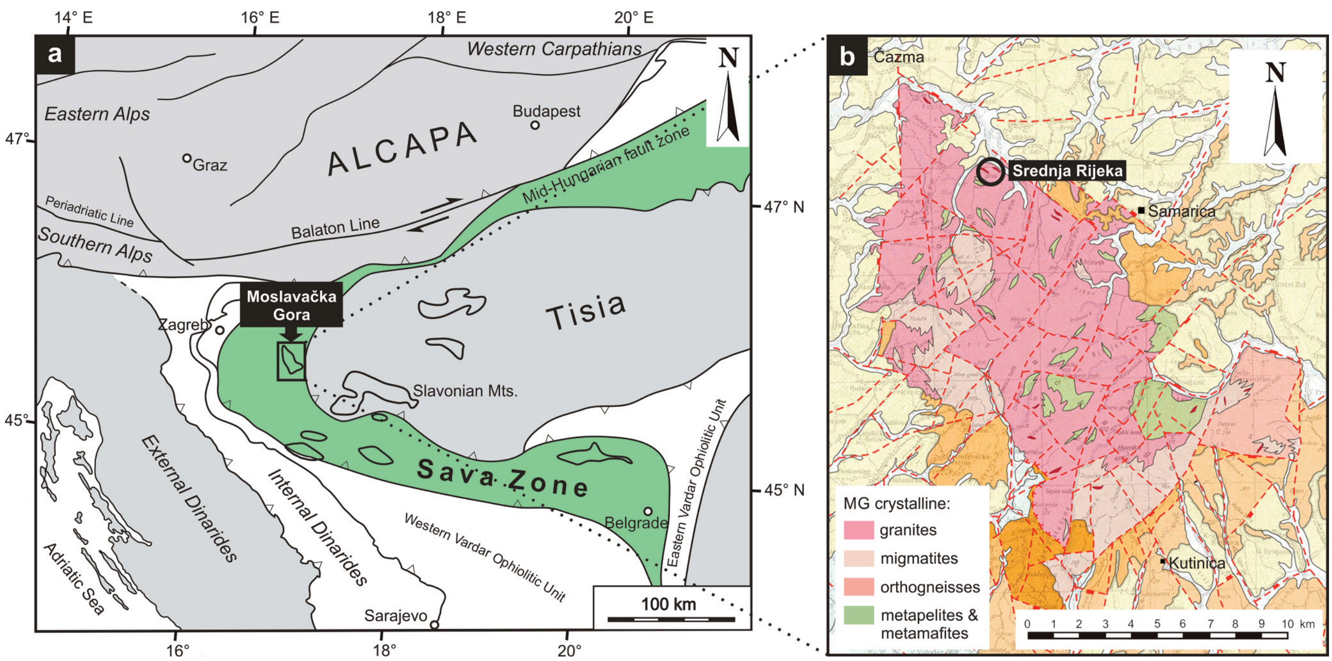

Fig. 1. *Simplified maps of:* ***(a)*** *the Dinaride–Alpine–Pannonian region showing the major structural units after* SCHMID *et al. (2008) and position of Moslavačka Gora (map is slightly modified after* LUŽAR-OBERITER *et al., 2012),* ***(b)*** *simplified geologic map of the Moslavačka Gora crystalline (modified after* KOROLIJA *&* CRNKO*, 1986;* CRNKO*, 1990;* PAMIĆ*, 1990) and position of the site with investigated tourmaline occurrences.*

nounced negative Eu anomaly (Eu/Eu* = 0.03–0.11 and 0.06–0.66), both showing significantly lower ΣREE (ΣREE=21.67–22.49 and 8.37–10.34 ppm) compared to two-mica granite (BALEN & BROSKA, 2011; BALEN & PETRINEC, 2011).

Previous studies of disseminated and nodular tourmaline occurrences used the granitoid host rocks from the type locality (Fig. 1b) (BALEN, 2007; BALEN & BROSKA, 2011; BALEN & PETRINEC, 2011). They are Late Cretaceous, as the overall dating of MG crystalline by different methods has already established (LANPHERE & PAMIĆ, 1992; BALEN et al., 2001, 2003; STARIJAŠ et al., 2010). The isotopic age of the studied leucogranite is constrained by the data of BALEN et al. (2001) to be 74±1.0 Ma (muscovite Ar–Ar). PALINKAŠ et al. (2000) also determined the Ar–Ar age on muscovite from the coarse-grained leucogranite with a plateau age of 73.2±0.8 Ma. They interpreted it as the age of muscovite crystallization and/or cooling.

The P-T conditions at the crystallization level of the two-mica granite were determined from the zircon saturation temperature and REE thermometry (ca. 720–730 °C). The combination of these temperatures and the Al_2SiO_5 phase diagram gave a pressure of 70–270 MPa (average depth ~5 km) (BALEN & BROSKA, 2011).

Our study focuses on known and specific occurrences of tourmaline from previously described granitoids from the Srednja Rijeka area on the northern margin of the MG crystalline. The first type of tourmaline, nodular tourmaline (NT), forms compact spherical aggregates (tourmaline nodules) within the two-mica granite. On the other hand, leucogranites often host prismatic crystals of disseminated tourmaline (DT) and radial aggregates of prismatic crystals (“tourmaline suns”) - Fig. 2. In this study, we present infrared measurements of tourmaline spectra for nodular and disseminated tourmalines separated from the two-mica granite and leucogranite host rocks, respectively. This study aims to use records from the O-H stretching region of IR spectra to investigate the role of fluids in the Late Cretaceous magmatic evolution of a complex Adria – Europe convergence zone during the final stages of host rock evolution. These records indi-

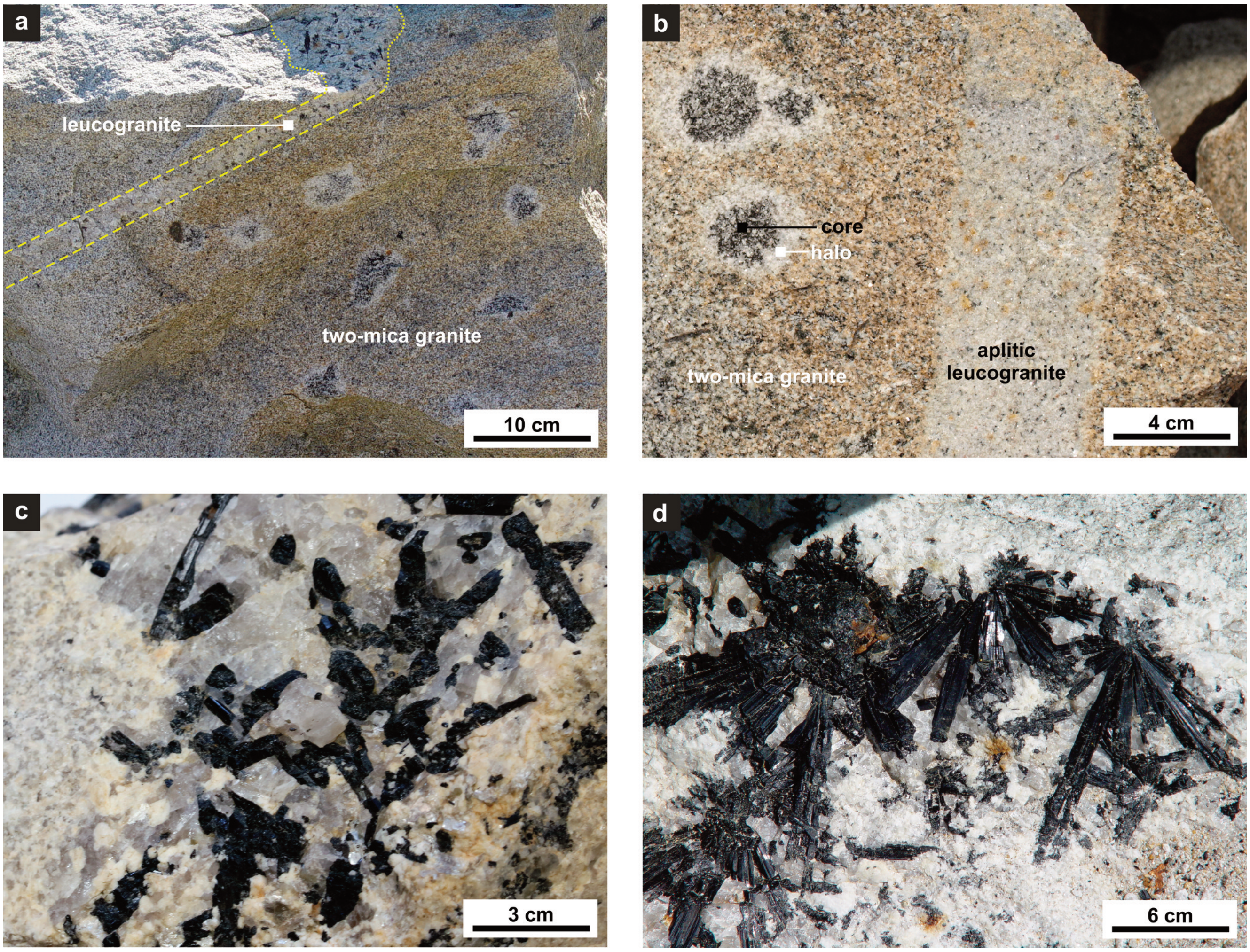

*Fig. 2. Tourmaline occurrences from MG: **(a)** contact of two-mica granite containing tourmaline nodules with leucogranite vein containing disseminated tourmaline grains; **(b)** typical occurrence of two-mica granite with spherical tourmaline nodules composed of a characteristic dark tourmaline-bearing core and a leucocratic rim (halo). Two-mica granite is cut by aplitic leucogranite; **(c)** Disseminated tourmaline crystals in the coarse-grained leucogranite; **(d)** radial aggregates of prismatic tourmaline crystals („tourmaline suns“).*

rectly point to changes in the tourmaline chemistry and reflect on the tourmaline structure, thus revealing the contrasting genesis and evolution of the studied tourmaline types.

Host rock petrography

Two-mica granite hosting tourmaline nodules exhibits either fine-grained equigranular or porphyritic textures (Fig. 2a, b). The mineral assemblage consists of quartz, plagioclase (albite to oligoclase), biotite, muscovite, and K-feldspar (orthoclase). At the same time, accessory phases include zircon, apatite, monazite, xenotime, and opaque mineral(s). Anhedral quartz grains are about 1 mm in size. Albite is tabular, similar in size to quartz, and randomly distributed in the rock. Mica flakes are 1–2 mm long but may form large clots up to 5 mm long. K-feldspar is also around 1 mm and is tabular in shape. Tourmaline nodules from two-mica granites typically occur as compact spherical to amoeboid aggregates, ranging from 1 to 10 cm in diameter. Tourmaline nodules from MG regularly exhibit a complex texture comprising two distinctly separated units: the tourmaline-bearing melanocratic core, which is enveloped by the leucocratic, biotite-free zone (halo). The tourmaline-bearing core consists of dravite-enriched, slightly Na-deficient tourmaline and quartz + albite + K-feldspar. The nodule halo, consisting of quartz + feldspar ± muscovite, is an integral part of the nodule and envelops the tourmaline-bearing core.

Leucogranites occur as smaller, irregular bodies and dykes cutting through two-mica granite. They are characterized by sharp to diffuse contacts towards the two-mica host (Fig. 2). They are generally characterized by subequal proportions of quartz, K-feldspar (microcline and orthoclase), and plagioclase (albite) with variable proportions of muscovite, biotite, garnet, andalusite, and tourmaline. Accessory minerals include apatite, zircon, and opaque phases. Quartz forms ~1 mm (in the fine-grained varieties) to one cm (in coarse-grained varieties) anhedral grains. Similar dimensions are characteristic for the feldspars (K-feldspar and plagioclase). Micas are scattered throughout the rock, with white mica (muscovite) predominating. Pink garnet forms anhedral interstitial grains reaching a few mm to a few cm in size. Black, elongated tourmaline grains, several mm to cm in size, are randomly distributed (i.e., disseminated) throughout the rock (Fig. 2c). Disseminated tourmaline (schorl) also occurs as "tourmaline suns" – radial aggregates of elongated schorl tourmaline crystals reaching up to 30 cm in diameter (Fig. 2d). Leucogranite texture varies between pegmatitic (grains a few mm to a few cm in size) and fine-grained (1–2 mm) aplitic.

Materials and method (FTIR spectroscopy)

Separation of 15 tourmaline samples, including samples of nodular tourmaline (NT) from two-mica granites (7 samples) and disseminated tourmaline crystals (DT) including radial aggregates ("tourmaline suns") from leucogranites (8 samples) was analyzed by FTIR spectroscopy. The IR spectral measurements from 4000 to 375 cm^{-1} with a resolution of 1 cm^{-1} (step) were performed at the Division of Mineralogy and Petrology, Department of Geology, Faculty of Science, University of Zagreb, using Bruker Tensor 27 infrared spectrometer. Samples were prepared from a powdered mixture of pure solid KBr and optically clear separation of tourmaline grains, which were pressed into a thin, transparent pellet. The approximate weight ratio of the sample to KBr was 1:100. Samples were prepared, and measurements were performed at room temperature. Data processing involved grouping the obtained spectra based on the details observed in the 3800–3100 cm^{-1} range. To avoid overlap of the IR spectra, one sample from each group was selected for graphical display in this contribution (DT 1 and NT 7). The resulting subdivision of tourmalines into two groups is consistent with the previously observed chemical differences between the studied tourmaline occurrences (Balen & Broska, 2011; Balen & Petrinec, 2011) and the results of the preliminary IR spectroscopic study reported by Balen et al. (2015).

Results

Differences in field occurrence and the chemistry of the studied tourmaline types reflect the complex crystal structure of tourmaline in general and consequently affect the properties of the infrared spectra. One of the most suitable regions for detecting differences between different types of tourmalines is the O-H stretching region (3800–3100 cm^{-1}).

The results of chemical analyses of tourmaline are given in Balen & Broska (2011) and Balen & Petrinec (2011). Based on their chemical characteristics, DT and NT tourmalines are defined as primary alkali group tourmalines (Henry et al., 2011), which differ in chemical composition: nodular tourmaline ranges from schorl to dravite (Fe# 0.43–0.58) and disseminated tourmaline is schorl (Fe#=0.75–0.85) – Table 1, Fig. 3.

Tourmaline spectra with emphasis on the O-H stretching region

Infrared spectra for representative disseminated (DT 1) and nodular (NT 7) tourmaline separations show typical groups of absorption bands consistent with the standard IR spectrum of tourmaline (e.g., schorl) from the RRUFF (2023) database. Many symmetrical absorption bands are found in the

Table 1. The structural formula of average values for nodular and disseminated tourmalines. The average is based on 14 selected analyses for each group. Data for calculation are taken from Balen & Broska (2011) and Balen & Petrinec (2011).

Tourmaline	X	Y	Z	T	V(O3)	W(O1)
Nodular (NT)	$Ca_{0.06}$ $Na_{0.59}$ $vac_{0.34}$ $K_{0.01}$	$Al_{0.43}$ $Mg_{1.18}$ $Fe^{2+}_{1.07}$	$Al_{6.00}$	$Si_{5.92}$ $Al_{0.08}$	(OH_3)	$OH_{0.99}$ $F_{0.01}$
Disseminated (DT)	$Ca_{0.02}$ $Na_{0.58}$ $vac_{0.39}$ $K_{0.01}$	$Al_{0.50}$ $Mg_{0.46}$ $Fe^{2+}_{1.73}$	$Al_{6.00}$	$Si_{5.90}$ $Al_{0.10}$	(OH_3)	$OH_{0.87}$ $F_{0.13}$

range 375–1000 cm^{-1}. The bands reflect the vibration of the $[Si_6O_{18}]$ group in the tourmaline structure caused by the bending vibration of Si-O, the symmetric stretching vibration of Si–O–Si, the symmetric stretching vibration of O–Si–O, the asymmetric stretching vibration of O–Si–O and the asymmetric stretching vibration of Si–O–Si, respectively.

The absorption bands around 1100–1000 cm^{-1} are assigned to MgOH bending, while the bands around 1300 cm^{-1} are assigned to the stretching vibration of (BO_3). Weak bands at around 3000 cm^{-1} in the sample DT 1 are associated with adsorbed water. The observation of four OH stretching bands in the hydroxyl stretching region (3800 to 3100 cm^{-1}) suggests mixed occupancy of octahedral sites in the studied tourmalines (e.g., Ertl, 2003, 2012; Frost, 2007; Zhao et al., 2012; Bačík, 2015; Fuchs et al., 2022; Li, 2022).

The spectra of the hydroxyl stretching region for the studied samples are shown in Fig. 5.

IR spectrum (Fig. 5) of the typical MG nodular tourmaline (NT 7) shows two asymmetric and relatively broad O-H stretching bands, whose observed positions are at 3635 cm^{-1} and 3554 cm^{-1}, with shoulders on the higher and lower wavenumber side. On the other hand, the IR spectrum of MG disseminated tourmaline (DT 1) shows four sharp O-H stretching bands: 3643 cm^{-1}, 3633 cm^{-1}, 3550 cm^{-1}, and 3484 cm^{-1}.

Discussion

Tourmaline minerogenesis in the context of host-rock petrogenesis

The minerals of the tourmaline supergroup are the most widespread and complex borosilicates, crystallizing in the R3m space group and occurring in a wide variety of rocks of different origins and compositions. The abundance and presence of tourmaline in different geologic systems made it an excellent candidate, often used to decipher crustal evolution (e.g., London, 2011; Dutrow & Henry, 2011; van Hinsberg et al., 2011; Bačík et al., 2018).

The two contrasting tourmaline occurrences in the Moslavačka Gora granite, disseminated schorl in leucogranite and dravite (grain rim and zone) to schorl (grain core) in tourmaline nodules from two-mica granite (Table 1, Fig. 3), indicate the independent origin of these phases as well as different evolution of their host rocks.

A preliminary model for the production of leucogranitic melts in the MG magmatic system based on geochemical studies (Garašić et al., 2007) indicates K-feldspar-rich melting residue and muscovite dehydration melting at low aH_2O. This model is related to the melting of continental crust in a collisional setting, which is at least partially consistent with field evidence and our observations. In the leucogranitic magmas, tourmaline is interpreted to be an early crystallizing phase, as evidenced by its euhedral shape with well-defined crystallographic forms and relatively homogeneous chemical composition (schorl). The origin of nodular tourmaline, which was the last mineral to crystallize in the evolved granitic system of Moslavačka Gora, was attributed to the interaction of a fluid phase from the residual granitic melt with the fluid originating from the wall-rock in the low-pressure crustal setting and relatively rapid cooling, resulting in increased MgO content (Balen & Broska, 2011).

Interpretation of the IR spectra O-H stretching region of MG tourmalines

The general tourmaline formula is $XY_3Z_6(T_6O_{18})(BO_3)_3V_3W$, where the most common

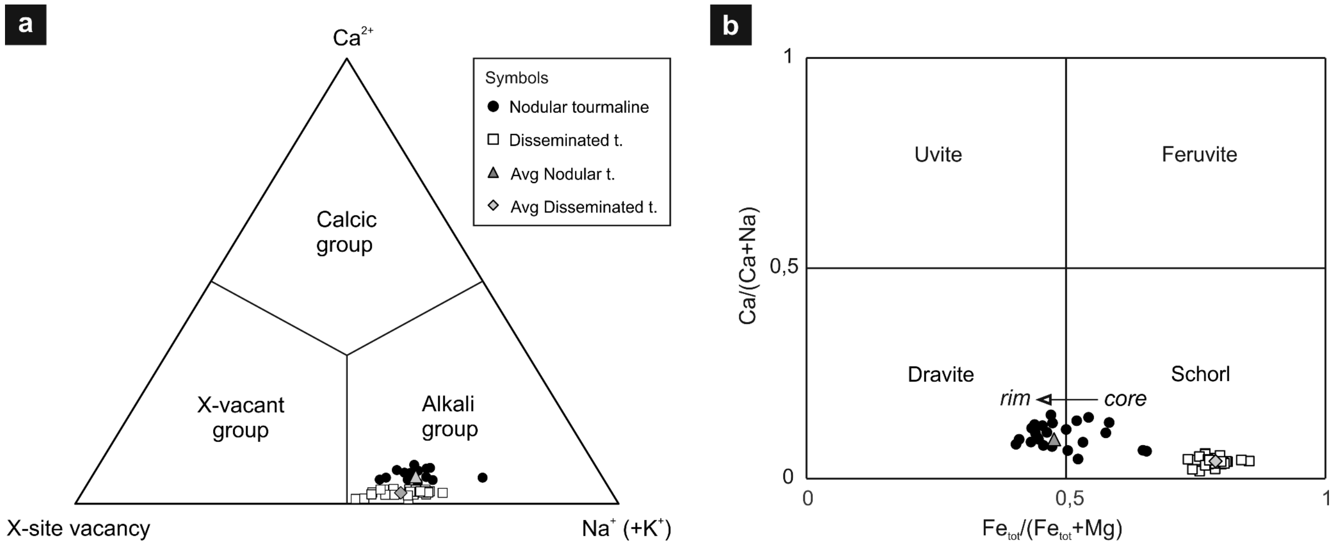

***Fig. 3. a)** Ternary system for the primary tourmaline groups based on the dominant occupancy of the X-site (Henry et al. 2011); **b)** Composition of different types of tourmaline plotted in terms of Ca/(Ca+Na) vs. $Fe_{tot}/(Fe_{tot}+Mg)$, graph after Baksheev et al. (2011). Data from Balen & Broska (2011) and Balen & Petrinec (2011).*

ions (or vacancy) at each site are: X = Na^+, Ca^{2+}, K^+, and vacancy; Y = Fe^{2+}, Mg^{2+}, Mn^{2+}, Al^{3+}, Li^+, Fe^{3+}, and Cr^{3+}; Z = Al^{3+}, Fe^{3+}, Mg^{2+}, and Cr^{3+}; T = Si^{4+}, Al^{3+}, and B^{3+}; B = B^{3+}; V = OH^- and O^{2-}; and W = OH^-, F^-, and O^{2-}.

In the tourmaline structure, the OH groups occupy two structurally distinct positions: the first position (OH_1, O1, W) is located in the center of the hexagonal rings, where the OH groups are coordinated by three Y octahedral cations. The second position (OH_3, O3, V) is located at the edge of the trigonal brucite-like fragments in the structure of tourmaline, and the OH groups are always coordinated by two Al cations and one Y cation. The highest frequency bands in the IR spectrum (above ~3600 cm^{-1}) correspond to the OH groups located in the hexagonal rings, whereas the bands in the 3600-3400 cm^{-1} region correspond to the OH groups located at the edge of the trigonal brucite-like fragments (e.g., Gonzalez-Carreño, 1988; Castañeda et al., 2000; de Oliveira et al., 2002; Skogby et al., 2012; Bosi et al., 2015a, b; Berryman et al., 2015; Bačík, 2018).

It is known that the presence of different cations near hydroxyl groups modifies the frequency of bands associated with OH in tourmalines. According to Gonzalez-Carreño (1988), the dravite-schorl series, in which the cations at the Y sites are predominantly Mg and Fe, is characterized by two bands centered at 3738 and 3633 cm^{-1}, the band with the higher frequency being more pronounced in dravites and the band with the lower frequency being more intense in schorls. In the infrared spectral region of 3600-3400 cm^{-1}, there is generally a unique component centered around 3550 cm^{-1}. The width of this component is greater in the case of schorl. According to Gonzalez-Carreño (1988), the observed components could be associated with Al Al Fe (3553–3558 cm^{-1}) and Al Al Al (3464–3494 cm^{-1}) environment. That interpretation fits well with the observations on MG tourmalines (Figs. 4, 5, Table 2).

The observed difference between the O-H stretching regions in the two tourmaline types and clearly defined absorption bands in both nodular and disseminated tourmalines from MG suggests different mineral evolution. The difference in evolution has implications for the cation distribution and results in subtle differences in OH coordination. The observation of OH stretching bands (although two of them are "hidden" in the broadband group of NT 7) in the hydroxyl stretching region corresponds to a mixed occupancy of octahedral sites in both tourmalines. The broadening observed in the lower wavenumber region of the NT 7 spectrum compared to the DT 1 spectrum suggests a higher water content associated with the crystallization of nodular tourmaline, while the observed shifts between the corresponding bands can be explained by the shortening of O-H_1 and O-H_3 distances, which are due to differences in petrogenetic processes, i.e., magmatic/hydrothermal (for NT) versus magmatic (for DT).

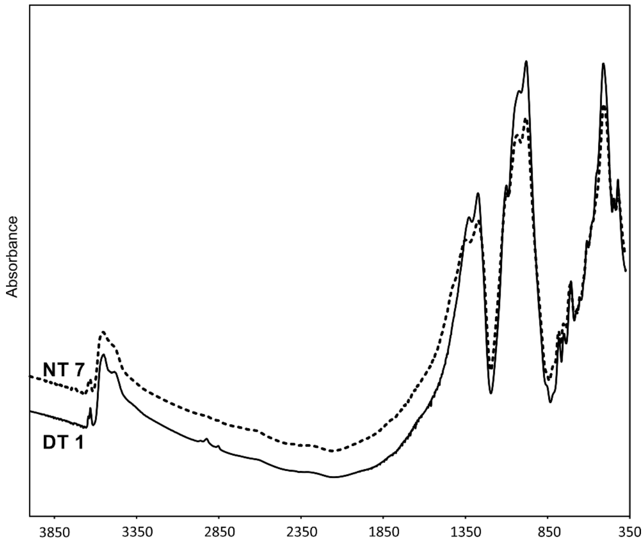

Fig. 4. IR spectra of nodular (NT 7, dotted line) and disseminated (DT 1, solid line) tourmalines in the 4000 to 375 cm⁻¹ region.

Table 2. Tourmaline O-H stretching bands were observed in the O-H stretching region (3800–3100 cm⁻¹). According to Zhang et al. (2008) and Bačik et al. (2011), a tentative cation assignment is given.

Tourmaline	Site		Tentative assignment at neighbor sites	Wavenumber (cm⁻¹)
Disseminated				
$\nu_1(OH_1)$	o1	W	$Al^YFe^YR^Y$	3643
$\nu_1(OH_1)$	o1	W	$Fe^YFe^YR^Y$	3633
$\nu_2(OH_3)$	o2	V	$(Fe, Al)^YAl^ZAl^Z$	3550
$\nu_3(OH_3)$	o3	V	$(Fe, Al)^YAl^ZAl^Z$	3484
Nodular				
$\nu_1(OH_1)$	o1	W	$Fe^YFe^YR^Y$	3635
$\nu_2(OH_3)$	o2	V	$(Fe, Mg, Al)^YAl^ZAl^Z$	3554
$\nu_3(OH_3)$	o3	V	$(Fe, Mg, Al)^YAl^ZAl^Z$	3488 (?)

R= Fe, Mg, Al, Mn

The O-H stretching region of the typical MG IR spectrum of nodular tourmaline from the two-mica granite (NT 7 in Fig. 5) is characterized by two

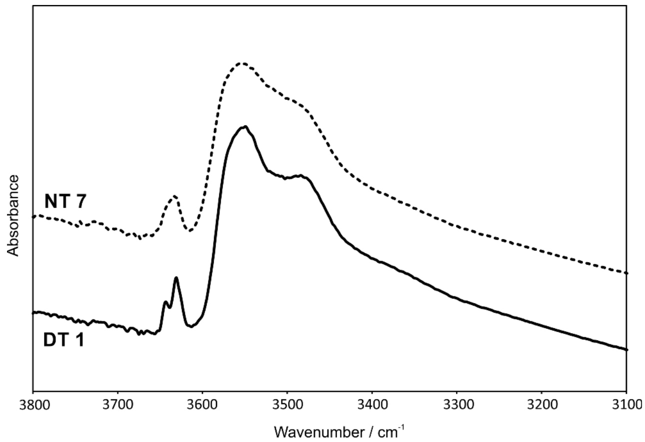

Fig. 5. O-H stretching region IR spectra (3800–3100 cm⁻¹) of the nodular (NT 7, dotted line) and disseminated (DT 1, solid line) tourmaline from Moslavačka Gora.

broad bands at 3635 and 3554 cm⁻¹. The band at 3554 cm⁻¹ is very broad and may have a shoulder on the low wavenumber side (~3488 cm⁻¹), which can be related to the third band at 3484 cm⁻¹ also observed in disseminated schorl tourmaline from leucogranites. However, the overall spectral behavior of NT tourmalines differs markedly from that of the DT tourmalines from leucogranites. The relatively weak vibrational bands above ~3600 cm⁻¹ can be assigned to the O1 site, while the strong bands below ~3600 cm⁻¹ can be assigned to the O3 site occupation (e.g. Skogby et al., 2012; Bosi et al., 2015a, b, 2016; Berryman et al., 2015). The observed minor variations in Fe, Mg, and Al content within MG tourmalines (Table 2) correlate with subtle variations in the band position. The broadening in the lower wavenumber region (Fig. 5) with an asymmetric band indicates lower crystallinity of the NT type and the important role of fluid-host rock interactions in controlling mineral chemistry (de Oliveira et al., 2000). This is consistent with general observations that tourmalines from more-evolved magmatic systems are well-crystallized and produce sharp bands, whereas tourmalines from less-evolved magmatic systems produce broad bands (e.g., Castañeda et al., 2000).

Conclusions

The present geological relations in the Moslavačka Gora crystalline reflect the complex history of magmatic evolution during several closely related events in the Late Cretaceous. The granite body itself shows evidence of at least two successive magmatic events – their signature was left behind in the form of different rock textures and relationships between known rock types, their mineral compositions, and geochemical characteristics, and in the shift of tourmaline composition from schorl to dravite.

The differences between the IR spectra of nodular (NT) and disseminated tourmaline (DT) are best seen in the O-H stretching region (3800–3100 cm^{-1}) of the infrared spectra. IR spectra of disseminated tourmaline show four sharp O-H stretching bands: 3643, 3633, 3550, and 3484 cm^{-1}, while nodular tourmaline shows asymmetric and relatively broad O-H stretching bands at 3635 and 3554 cm^{-1} with shoulders on the higher and lower wavenumber side. The OH stretching bands have been studied in detail because of their sensitivity to crystallochemical features controlled partly by the bulk chemistry, the water content in the system, rock-fluid interaction, degree of "crystallinity," geologic history or magma evolution, and temperature-pressure conditions. The broadening in the lower wavenumber range compared to disseminated tourmaline suggests a higher water content in nodular tourmaline, while the observed shifts between the corresponding bands can be explained by shortening of the $O\text{-}H_1$ and $O\text{-}H_3$ distances, which can be attributed to different formation (geological) processes.

The origin of nodular tourmaline, which was the last mineral to crystallize in the evolved Late Cretaceous granite system of Moslavačka Gora, is attributed to the interaction of a fluid phase from the residual granitic melt with fluid originating from the wall rock in the low-pressure crustal setting, which was supported by relatively rapid cooling, resulting in increasing dravite content in nodular tourmaline toward the nodule margin. Disseminated tourmaline from the leucogranite can be considered a typical magmatic (pegmatitic) product and a common accessory phase in leucogranites.

Acknowledgments

This work has been partly supported by the Croatian Science Foundation under project number IP-2014-9541. The authors are grateful to the GABP editor(s) and the reviewers (V. Cvetković and D. Srećković-Batoćanin) for their constructive comments and suggestions.

References

Bačík, P. 2015. Cation ordering in octahedral sites in tourmalines of schorl-dravite series. *Canadian Mineralogist*, 53: 571–590.

Bačík, P. 2018. The crystal-chemical autopsy of octahedral sites in Na-dominant tourmalines: octahedral metrics model unconstrained by the Y, Z-site disorder assignment. *Journal of Geosciences*, 63: 137–154.

Bačík, P., Ozdín, D., Miglierini, M., Kardošová, P., Pentrák, M. & Haloda, J. 2011. Crystallochemical effects of heat treatment on Fe-dominant tourmalines from Dolní Bory (Czech Republic) and Vlachovo (Slovakia). *Physics and Chemistry of Minerals,* 38: 599–611.

Bačík, P., Uher, P., Dikej, J. & Puškelová, Ľ. 2018. Tourmalines from the siderite-quartz-sulphide hydrothermal veins, Gemeric unit, western Carpathians, Slovakia: crystal chemistry and evolution. *Mineralogy and Petrology*, 112: 45–63.

Baksheev, I.A., Prokof'ev, V.Y., Yapaskurt, V.O., Vigasina, M.F., Zorina, L.D. & Solov'ev, V.N. 2011. Ferric-iron-rich tourmaline from the Darasun gold deposit, Transbaikalia, Russia. *Canadian Mineralogist*, 49 (1): 263–276.

Balen, D. 2007. Tourmaline nodules occurrences in Moslavačka Gora (Croatia) granite: a snapshot of magmatic processes. *8th Workshop on Alpine Geological Studies*, 3–3.

Balen, D. & Broska, I. 2011. Tourmaline nodules – products of devolatilization within the final evolutionary stage of granitic melt? *In:* Sial, A. N., Bettancourt, J.S., De Campos, C.P. & Ferreira, V.P. (Eds.). *Granite-Related Ore Deposits*. Geological Society London Special Publications, 350: 53–68.

Balen, D. & Petrinec, Z. 2011. Contrasting tourmaline types from peraluminous granites: a case study from Moslavačka Gora (Croatia). *Mineralogy and Petrology*, 102: 117–134.

Balen, D., Schuster, R., & Garašić, V. 2001. A new contribution to the geochronology of Mt. Moslavačka Gora (Croatia). *In:* Ádam, A., Szarka, L. & Szendrői, J. (Eds.). *PANCARDI 2001*, 2–3.

Balen, D., Schuster, R., Garašić, V. & Majer, V. 2003. The Kamenjača olivine gabbro from Moslavačka Gora (South Tisia, Croatia). *Rad Hrvatske akademije znanosti i umjetnosti*, 486: 57–76.

Balen, D., Petrinec, Z. & Juranić, V. 2015. Infrared study of O-H stretching region in the nodular and disseminated dravite-schorl series tourmalines from Moslavačka gora (Croatia). *5th Croatian Geological Congress Abstracts book*, 22–23.

Berryman, E.J., Wunder, B., Ertl, A., Koch-Müller, M., Rhede, D., Scheidl, K., Giester, G. & Heinrich, W. 2015. Influence of the X-site composition on tourmaline's crystal structure: Investigation of synthetic K-dravite, dravite, oxy-uvite, and magnesio-foitite using SREF and Raman spectroscopy. *Physics and Chemistry of Minerals*, 43: 83–102.

Bosi, F., Skogby, H., Lazor, P. & Reznitskii, L. 2015a. Atomic arrangements around the O3 site in Al- and Cr-rich oxy-tourmalines: a combined EMP, SREF, FTIR and Raman study. *Physics and Chemistry of Minerals*, 42: 441–453.

Bosi, F., Andreozzi, G.B., Hålenius, U. & Skogby, H. 2015b. Experimental evidence for partial Fe^{2+} disorder at the Y and Z sites of tourmaline: a combined EMP, SREF, MS, IR and OAS study of schorl. *Mineralogical Magazine*, 79: 515–528.

Bosi, F., Skogby, H. & Balić-Žunić, T. 2016. Thermal stability of extended clusters in dravite: a combined EMP, SREF and FTIR study. *Physics and Chemistry of Minerals*, 43: 395–407.

Castañeda, C., Oliveira, E.F., Gomes, N. & Soares, A.C.P. 2000. Infrared study on OH sites in tourmaline from the elbaite-schorl series. *American Mineralogist*, 85: 1503–1507.

Chappell, B.W. & White, A.J.R. 1974. Two Contrasting Granite Types. *Pacific Geology*, 8: 173–174.

Crnko, J. 1990. Osnovna geološka karta Republike Hrvatske 1:100 000. List Kutina L 33-94 [*Basic Geologic Map of Republic of Croatia 1:100 000. Sheet Kutina L 33-94*]. Hrvatski geološki institut, Zagreb.

Crnko, J. & Vragović, M. 1990. Osnovna geološka karta Republike Hrvatske 1:100 000. Tumač za list Kutina L 33-94 [*Basic Geologic Map of Republic of Croatia 1:100 000. Explanatory booklet for the Sheet Kutina L 33-94 – in Croatian*]. Hrvatski geološki institut, Zagreb, 75 pp.

Dutrow, B.L. & Henry, D.J. 2011. Tourmaline: A geologic DVD. *Element*s, 7: 301–306.

Ertl, A., Hughes, J.M., Brandstätter, F., Dyar, M.D. & Prasad, P.S.R. 2003. Disordered Mg-bearing olenite from a granitic pegmatite at Goslarn, Austria: a chemical, structural, and infrared spectroscopic study. *Canadian Mineralogist*, 41 (6): 1363–1370.

Ertl, A., Kolitsch, U., Dyar, M.D., Hughes, J.M., Rossman, G.R., Pieczka, A., Henry, D.J., Pezzotta, F., Prowatke, S., Lengauer, C.L., Körner, W., Brandstätter, F., Francis, C.A., Prem, M. & Tillmanns, E. 2012. Limitations of Fe^{2+} and Mn^{2+} site occupancy in tourmaline: Evidence from Fe^{2+}- and Mn^{2+}-rich tourmaline. *American Mineralogist*, 97: 1402–1416.

Frost, R., Wain, D., Reddy, J., Martens, W. & Kloprogge, T. 2007. Spectroscopic characterization of Mn-rich tourmalines. *Vibrational Spectroscopy*, 44 (1): 42–49.

Fuchs, Y., Fourdrin, C. & Balan, E. 2022. Theoretical OH stretching vibrations in dravite. *European Journal of Mineralogy*, 34: 239–251.

Garašić, V., Kršinić, A., Schuster, R. & Vrkljan, M. 2007. Leucogranite from Srednja Rijeka (Moslavačka Gora, Croatia). *8th Workshop on Alpine Geological Studies*, 21–21.

Gonzalez-Carreño, T., Fernandez, M., & Sanz, J. 1988. Infrared and electron microprobe analysis in tourmalines. *Physics and Chemistry of Minerals*, 15: 452–460.

Henry, D.J., Novak, M., Hawthorne, F.C., Ertl, A., Dutrow, B.L., Uher, P. & Pezzotta, F. 2011. Nomenclature of the tourmaline-supergroup minerals. *American Mineralogist*, 96: 895–913.

Korolija, B. & Crnko, J. 1986. Osnovna geološka karta SFRJ 1:100 000. List Bjelovar L 33-82. [*Basic Geologic Map of SFR Yugoslavia 1:100 000. Sheet Bjelovar L 33-82*]. Savezni geološki zavod, Beograd.

Korolija, B., Vragović, M., Crnko, J. & Mamužić, P. 1986. Osnovna geološka karta SFRJ 1:100 000, Tumač za list Bjelovar L 33-82 [*Basic Geologic Map of SFR Yu-*

goslavia 1:100 000. Explanatory booklet for the Sheet Bjelovar L 33-82 – in Serbo-Croatian]. Savezni geološki zavod, Beograd, 52 pp.

Lanphere, M. & Pamić, J. 1992. K-Ar and Rb-Sr ages of Alpine granite-metamorphic complexes in the northwestern Dinarides and the southwestern part of the Pannonian Basin in northern Croatia. *Acta Geologica Zagreb*, 22: 97–111.

Li, M. 2022. Spectroscopic characteristics and color origin of red tourmaline from Brazil. *Journal of Spectroscopy*, 1769710.

London, D. 2011. Experimental synthesis and stability of tourmaline: A historical perspective. *Canadian Mineralogist*, 49: 117–136.

Lužar-Oberiter, B., Mikes, T., Dunkl, I., Babić, Lj. & von Eynatten, H. 2012. Provenance of Cretaceous synorogenic sediments from the NW Dinarides (Croatia). *Swiss Journal of Geosciences*, 105: 377–399.

de Oliveira, E.F., Castañeda, C., Eeckhout, S.G., Gilmar, M.M., Kwitko, R.R., de Grave, E. & Botelho, N.F. 2002. Infrared and Mössbauer study of Brazilian tourmalines from different geological environments. *American Mineralogist*, 87: 1154–1163.

Palinkaš, A.L., Balogh, K., Strmić, S., Pamić, J. & Bermanec, V. 2000. Ar/Ar dating and fluid inclusion study of muscovite, from the pegmatite of Srednja Rijeka, within granitoids of Moslavačka gora Mt., North Croatia. *In:* Tomljenović, B., Balen, D. & Saftić, B. (Eds.). *PANCARDI 2000 Special Issue*. Vijesti Hrvatskog geološkog društva, 37: 95–96.

Pamić, J. 1990. Alpine granites, migmatites and metamorphic rocks from Mt. Moslavačka Gora and the surrounding basement of the Pannonian Basin (Northern Croatia, Yugoslavia). *Rad Jugoslavenske akademije znanosti i umjetnosti*, 10: 7–121.

Pamić, J. 1993. Eoalpine to Neoalpine magmatic and metamorphic processes in the northwestern Vardar Zone, the easternmost Periadriatic Zone and the southwestern Pannonian Basin. *Tectonophysics*, 109: 273–307.

Pamić, J. 2002. The Sava-Vardar Zone of the Dinarides and Hellenides versus the Vardar Ocean. *Eclogae Geologicae Helvetiae*, 95: 99–113.

RRUFF 2023. Schorl R050304. http://rruff.info/schorl/source/asc/R050304

Schmid, S.M., Bernoulli, D., Fügenschuh, B., Matenco, L., Schefer, S., Schuster, R., Tischler, M. & Ustaszewski, K. 2008. The Alps–Carpathians–Dinarides connection: a compilation of tectonic units. *Swiss Journal of Geosciences*, 101: 139–183.

Schmid, S.M., Fügenschuh, B., Kounov, A., Maţenco, L., Nievergelt, P., Oberhänsli, R., Pleuger, J., Schefer, S., Schuster, R., Tomljenović, B., Ustaszewski, K. & van Hinsbergen, D.J.J. 2020. Tectonic units of the Alpine collision zone between Eastern Alps and western Turkey. *Gondwana Research*, 78: 308–374.

Skogby, H., Bosi, F., & Lazor, P. 2012. Short-range order in tourmaline: a vibrational spectroscopic approach to elbaite. *Physics and Chemistry of Minerals*, 39, 811–816.

Spahić, D. 2022. The birth of the Sava Suture Zone: The early geological observations and the context of bimodal magmatism (southern Belgrade outskirts; Anđelković, 1973). *Geološki anali Balkanskoga poluostrva*, 83 (1): 23–37.

Spahić, D. & Gaudenyi, T. 2022. On the Sava Suture Zone: Post-Neotethyan oblique subduction and the origin of the Late Cretaceous mini-magma pools. *Cretaceous Research*, 131: 105062.

Starijaš, B., Gerdes, A., Balen, D., Tibljaš, D. & Finger, F. 2010. The Moslavačka Gora crystalline massif in Croatia: a Cretaceous heat dome within remnant Ordovician granitoid crust. *Swiss Journal of Geosciences*, 103: 61–82.

van Hinsberg, V.J., Henry, D.J., & Marschall, H.R. 2011. Tourmaline: An ideal indicator of its host environment. *Canadian Mineralogist*, 49: 1–16.

Zhang, A., Wang, R., Li, Y., Hu, H., Lu, X., Ji, J. & Zhang, H. 2008. Tourmalines from the Koktokay No. 3 pegmatite, Altai, NW China: spectroscopic characterization and relationships with the pegmatite evolution. *European Journal of Mineralogy*, 20: 143–154.

Zhao, C., Liao, L., Xia, Z., & Sun, X. 2012. Temperature-dependent Raman and infrared spectroscopy study on iron-magnesium tourmaline with different Fe content. *Vibrational Spectroscopy*, 62: 28–34.

Резиме

Студија инфрацрвеног спектра турмалина Мославачке горе (Хрватска) из подручја O-H растезања (stretching): значај флуида у горњокредној магматској еволуцији комплексне зоне конвергенције Адриа – Европа

Садашњи геолошки односи у кристалину Мославачке горе одражавају сложену магматску еволуцију током неколико блиско повезаних догађаја у касној креди. Кристалин Мославачке горе састоји се од магматских стијена (углавном гранита) уз које се јављају метаморфне стијене средњег до високог ступња метаморфизма. Само гранитно тијело показује доказе о најмање два узастопна магматска догађаја који су резултирали настанком двотињчастог гранита, као преовладавајућег типа, те леукогранита, као другог најзаступљенијег типа мославачких гранита. Ти су догађаји оставили видљиве потписе у различитим текстурним карактеристикама ових стијена, њиховим теренским односима, минералном саставу и геокемијским обиљежјима, као и у промјени састава минерала турмалина од шерла (schorla) према дравиту. Двотињчасти гранит садржи специфична сферична тијела – турмалинске нодуле – у чијој се језгри јавља нодуларни турмалин, док су турмалини у леукогранитима присутни као дисеминирани субхедрални кристали.

Разлике између IR спектара нодуларног (NT) и дисеминираног турмалина (DT) најбоље се опажају у подручју O-H растезања IR спектра (3800–3100 cm^{-1}). IR спектри дисеминираног турмалина показују четири уске врпце O-H растезања: 3643, 3633, 3550 и 3484 cm^{-1}, док нодуларни турмалин показује асиметричне и релативно широке врпце O-H растезања на 3635 и 3554 cm^{-1}, с проширењима на вишим и нижим валним бројевима. Врпце O-H растезања су детаљно проучаване због њихове осјетљивости на кристалокемијске карактеристике, које су пак дјеломично контролиране укупним кемијским саставом, садржајем воде присутне у суставу, интеракцијом стијена и флуида, ступњем „кристалинитета“, геолошком повијести и/или еволуцијом магме те увјетима температуре и тлака. Проширење врпци у подручју нижег валног броја опажено је код нодуларног турмалина, што указује на виши садржај воде у нодуларном турмалину у односу на дисеминирани турмалин. Уочени релативни помаци између одговарајућих врпци код нодуларног у односну дисеминирани тип турмалина могу се објаснити скраћивањем O-H_1 и O-H_3 размака, што се може приписати различитим генетским и/или еволуцијским процесима.

Поријекло нодуларног турмалина приписује се међудјеловању флуидне фазе из резидуалне гранитне магме с флуидом поријеклом из околних стијена у увјетима ниског тлака плитко у кори, те је он кристализирао као посљедњи минерал у еволуираном суставу каснокредних гранита Мославачке горе. Ови су процеси били подржани релативно брзим хлађењем, што је резултирало повишењем садржаја дравита у нодуларном турмалину, гледано од средишта према рубу нодула. За разлику од тога, дисеминирани турмалин (по саставу schorl) из леукогранита може се сматрати типичним магматским (пегматитским) продуктом и уобичајеном акцесорном фазом у леукограниту.

Manuscript received March 01, 202
Revised manuscript accepted May 22, 2023